

Exosome-mediated transfer of microRNAs promotes mouse iPSCs differentiation into therapeutic insulin-producing cells

Qingsong Guo (✉ ntgglj@163.com)

Affiliated Hospital of Nantong University <https://orcid.org/0000-0001-5194-2370>

Yuhua Lu

Affiliated Hospital of Nantong University

Yan Huang

Affiliated Hospital of Nantong University

Yibing Guo

Affiliated Hospital of Nantong University

Shajun Zhu

Affiliated Hospital of Nantong University

Qiuqiang Zhang

Affiliated Hospital of Nantong University

Donghui Zhu

Nantong University Medical School

Zhiwei Wang (✉ wzw3639@163.com)

Affiliated Hospital of Nantong University

Jia Luo (✉ tdfylj@163.com)

Affiliated Hospital of Nantong University

Research Article

Keywords: diabetes, exosomes, iPSCs, differentiation, miRNA, insulin

Posted Date: June 18th, 2021

DOI: <https://doi.org/10.21203/rs.3.rs-561531/v1>

License: © ⓘ This work is licensed under a Creative Commons Attribution 4.0 International License.

[Read Full License](#)

Abstract

Purpose

Exosome-based therapeutic approaches have been applied in diabetes. In the present study, we explored the effect of exosomes on iPSCs differentiation into insulin-producing cells and its underlying mechanisms.

Methods

Exosomes were isolated by ultracentrifugation from MIN6 cells and identified by Transmission electron microscopy (TEM), nanoparticle tracking analysis (NTA) and Western blot. PKH67 tracer and transwell assay were used to confirm exosome delivery into iPSCs. QRT-PCR was applied to detect key pancreatic gene expression and miRNAs expression in differentiated iPSCs. Insulin expression was assessed by flow cytometry (FCM) and immunofluorescence. The mechanism underlying exosome induction capacity for iPSCs was determined via RNA-interference of Argonaute-2 (Ago2). Streptozotocin (STZ) was used to establish diabetic mouse model to verify the function of differentiated β -like cells.

Results

MIN6-derived exosomes promoted the key pancreatic gene expression and immunofluorescence for Nkx6.1 and insulin remarkably, confirming the capability of exosomes for iPSCs differentiation. Moreover, transplantation of differentiated iPSCs efficiently enhanced IPGTT and partially control hyperglycemia in T1D mice. Knockdown of Ago2 in MIN6 cells affect exosomal miRNAs expression and pancreatic gene expression and insulin secretion in iPSCs. The therapeutic effect in vivo was weakened, further indicating decreased exosomal miRNA affect iPSCs differentiation. 7 specific exosomal miRNAs were selected for single-assay validation. MiR-706, miR-709, miR-466c-5p and miR-423-5p were found dynamic changed during differentiation stages.

Conclusion

Exosomes is an effective and convenient induction approach for iPSCs differentiation into functional insulin secreting cells. The effect was downregulated via Ago2 knockdown illustrates the mechanisms are highly relevant to specific miRNAs enriched in exosomes.

Introduction

Diabetes is one of the most common chronic disease worldwide, mainly characterized by the dysfunction of pancreatic islets or the loss of insulin-producing β cells^[1]. The incidence of diabetes has rapidly risen

in recent years^[2, 3]. Replenishment or regeneration of the destroyed pancreatic islet β -cells by appropriate alternative cells to restore β -cell function was an ideal clinical treatment. Although the application of pancreas and islet transplantation has provided an opportunity to cure diabetes^[4, 5], the approach applied in clinical treatments are still impaired by lack of donor sources, functionality of isolated pancreatic islets from donors and immune rejection^[6, 7]. In order to overcome the existed shortcomings, stem cell derived β -cell therapy has been proposed as a feasible solution.

It was reported that iPSCs can be differentiated into IPCs in vitro and used as an alternative source for transplanting β cells^[1], sequential treatments with exogenous molecules were applied to induce differentiation from iPSCs. However, some DNA-based reprogramming techniques may bring biosafety problem, such as insertional mutagenesis or tumorigenesis. On the other hand, the functionality and maturity of iPCs is still low^[8]. Therefore, to construct an efficient induction approach for iPSCs differentiated into functional insulin producing cells sparks many research efforts in recent years.

Exosomes are microvesicles of 30-150nm of diameter that originate from the late endosomal pathway, with endocytic-derived structures surrounded by a phospholipid bi-layer that can be secreted into the extracellular space, transferring bioactive components among cells^[9]. Intercellular delivery of exosomes plays an important role in modifying or reprogramming the phenotype of recipient cells^[10]. Pancreatic islets and different β -cell lines have been reported to release exosomes^[11-13]. The function of β -cell exosomes is just beginning to unfold, but there is already evidence indicating that these extracellular vesicles participate in the cross talk with stem cells differentiation.

Particular microRNAs are selectively packaged into exosomes and transferred to recipient cells, playing critical roles in post-transcriptional regulation of related gene expression and affect the differentiation process^[14]. During islet development, miRNAs directly or indirectly target islet cell specific genes, resulting in translational repression or mRNA degradation, thus regulating islet cell differentiation and maturation^[15-18]. Ago2 is integral to miRNA function as well as to the packaging of miRNA into exosomes^[19-21]. It is reported that the function of exosomal miRNA is dependent on Ago2 derived from the donor cells instead of recipient cells. Therefore, knockdown of Ago2 in host cells allows the isolation and testing of miRNA-depleted exosomes^[22, 23]. So far, the possible contribution of exosomal miRNAs in the distant signaling on iPSCs differentiation into insulin-producing cells (iPCs) has not been fully elucidated. Here, we aimed to test the differentiation potential of MIN6 cell-derived exosomes on iPSCs in vitro and to explore whether the effect is miRNA-dependent. The identification of these miRNAs would help us better understand the molecular events and the mechanism involved in such differentiation process, and further improve the potential of islet tissue regeneration engineering.

Materials And Methods

Cell culture

The MIN6 cell line was purchased originally from ATCC maintained in DMEM supplemented with 10% (v/v) exosome-depleted FBS (Gibco, Grand Island, NY, USA), 100 U/ml penicillin and 100 µg/ml streptomycin and cultured at 37°C in a 5% CO₂ incubator. The iPSCs induced via a three-step protocol in our laboratory^[24] at Multi-lineage pluripotent cells (MPC) stage was maintained in DMEM/F12 conditioned medium with 10% (v/v) FBS, 100 U/ml penicillin and 100 µg/ml streptomycin. Cells were cultured in differential medium prepared with high glucose-DMEM (H-DMEM, Gibco) with or without exosomes purified from MIN6 cells. The culture medium was changed twice a day for a total 21 days.

Exosomes isolation

Exosomes were isolated from conditioned medium of MIN6 cells culture media. The cell culture media was centrifuged at 2000 *g* for 10 min at 4°C and spun again at 11,000 *g* for 30 min at 4°C. The supernatant was filtered through a 0.22 µm filter (Millipore-sigma). Ultracentrifugation was performed at 150,000 *g* for 2h at 4°C followed by an additional washing with PBS at 150,000 *g* for 90 minutes. All the pellets collected were resuspended in 100µl PBS and stored at -80°C for further experiments. Exosomes were diluted in iPSCs culture medium to a final volume corresponding to 1:5 of the original MIN6 culture volume.

Exosomes identification and quantification

TEM was applied to observe the morphology of particles in the pellets. In brief, 10 µl exosomes suspension was placed on to formvar/carbon-coated nickel TEM grids and incubated for 30 min. The grids were then washed, dried and imaged using an H-7650 transmission electron microscope (HITACHI, Japan) to identify the morphology.

NTA was carried out using the LM10 Nanosight (Malvern) equipped with a sample chamber and a 405 nm laser. Exosomes were diluted in PBS to fit in the resolution window of measurement suggested by the instrument manufacturer. Three separate fields of view were captured for each sample for 30s measurements at room temperature. The Nanosight NTA 3.1 software was used to capture and analyze the particles.

Ago2 inactivation in MIN6 cells with siRNA against Argonaut-2 (siAgo2)

MIN6 cells were transfected with Ago2 using Lipofectamine 3000 (Sigma-Aldrich) according to the manufacturer's protocol. Briefly, 80% confluent MIN6 cells were incubated with Lipofectamine 3000 reagent and siAgo2 or a scrambled control siRNA (siNC) for 48h. QPCR and western blot were applied to verify interference efficiency.

Exosomes labeling and uptaking by iPSCs

Exosomes were labeled with PKH67 Green Fluorescent Cell Linker Kit (Sigma-Aldrich) according to the manufacturer's protocol with minor modifications. The labeled exosomes were washed at 150,000 *g* for

1h and diluted in 100 μ l PBS and added into the iPSCs culture medium for the uptake experiments. Transwell (Corning) was also applied to co-culture MIN6 cells with iPSCs. MIN6 cells were seeded in the top inserts placed into 24-well culture plates seeded with iPSCs. The transfection reagent si-transfect-Cy3 for siRNA positive control was transfected into MIN6 cells. Fluorescence in MIN6 cells were detected after 24h and iPSCs after 48 h respectively with Fluorescence Microscope.

RNA extraction and quantitative RT-PCR analysis

Total RNA was extracted using Trizol and the first-strand cDNA synthesis for Ago2 and other genes were performed using the RevertAid First Strand cDNA Synthesis Kit (Roche) following the manufacturer's instructions. The relative expression levels of each mRNA were calculated by the $2^{-\Delta\Delta C_t}$ method as previously described, and GAPDH was used as control (U6 was used as control for miRNAs). Each experiment was performed independently and repeated three times. The qRT-PCR primer sequences were designed and synthesized by Ruibo Biotech Corp. (Guangzhou, China). Sequences of the primers are shown in Table 1.

Immunofluorescence

Cells on glass coverslips were washed with pre-cooling PBS and fixed with 4% paraformaldehyde for 15min at room temperature, permeabilized with 0.5% (v/v) Triton X-100. 5% BSA was incubated for 1h and co-incubated with specific primary antibodies at 4°C overnight. Cells were stained with fluorescence secondary antibodies and hocheist (Thermo Fisher Scientific). Primary antibodies are listed as follows: anti-insulin antibody (Abcam), anti-NKX6.1 rabbit mAb (Cell Signaling Technology), anti-glucagon antibody (Abcam) . Secondary antibodies included donkey anti-rabbit (Alexa Fluor® 555, Abcam), goat anti-guinea pig (Alexa Fluor® 647, Abcam).

Flow cytometry

FCM was applied to identify the insulin-positive population. 1×10^6 differentiated iPSCs on day7, day 14 were digested with 0.25% trypsin, washed and resuspended as single cells by incubation in Reagent 1: Fixation (Beckman Coulter). Then, cells incubated in Reagent 2: Permeabilization (Beckman Coulter) and washed. Next, cells were resuspended in PBS with primary antibody and incubated for 30 min, then washed and analyzed with the BD FACSCalibur system (BD Biosciences). The primary antibody was anti-h/b/m insulin APC-conjugated rat IgG2A (R&D Systems). The isotype antibody was rat IgG2A control APC-conjugated.

Western blot

Proteins from exosomes and cell lysates were migrated on SDS-PAGE, transferred to PVDF membranes (Millipore, Bedford, MA, USA), blocked with 5% skim milk and probed with primary antibodies against Alix, TSG101, Ago2 or β -actin in Antibody Dilution Buffer at 4°C overnight. The membranes were incubated with HRP-conjugated secondary antibodies after washing with TBST. The blots were then developed by

using ECL kit (Thermo Fisher Scientific). Densitometry of immunoblotting bands was quantified by using the Multi Gauge software V3.0 from Fuji Film (Minato, Tokyo, Japan).

Animals

C57BL/6J male mice were from the Laboratory Animal center of Nantong University. Mice were injected with a single intraperitoneal of 200 mg/kg STZ, non-fasting blood glucose levels in the tail vein were monitored continuously. Two weeks later, 24 mice with high blood glucose (>14.4mg/mL) were randomly divided into STZ +iPSCs group, STZ+exosome-induced iPSCs and STZ+siAgo2-exosome-induced iPSCs (n=8). 1×10^7 iPSCs induced with exosomes for 21 days were implanted under the right renal capsule. Blood glucose were measured before and after transplantation. After fasting for 8 hours on the 7th–14th and 21st day after transplantation, the intraperitoneal glucose tolerance test (IPGTT) was performed by intraperitoneal injection of 10% glucose solution (2mg/kg). All animal experiments were performed according to the Institutional Animal Care guidelines and were approved by the Animal Ethics Committee of Nantong University.

Statistical analysis

Data are analyzed by Graphpad 10.0. ANOVA analysis was performed for comparisons of three or more groups and presented as the mean \pm standard deviation (SD). $p < 0.05$ was considered statistically significant.

Results

Isolation and characterization of exosomes released by MIN6 cells

Exosomes released by MIN6 cells were isolated by ultra-centrifugation and characterized for their size (Fig 1A). Alix and TSG101, typical markers of exosomes, were highly expressed (Fig 1B). TEM images was performed on the samples re-suspended in TBS and revealed a diverse population of particles (Fig 1C). Using nanoparticle tracking analysis, the purified microvesicles were mainly enriched from 60 nm to 200 nm in diameter with an average size of 140.3 nm (Fig 1D).

MIN6-derived exosomes successfully integrated and delivered cargos to iPSCs

To reveal exosome uptake mechanisms by iPSCs, purified exosomes labeled with the green fluorescent marker PKH67 were incubated with iPSCs. PKH67-labeled exosomes were actually incorporated into iPSCs 24h later (Fig 2A).

Next, a transwell co-culture assay system with 0.4- μ m porous membrane was applied to study the crosstalk between MIN6 cells and iPSCs. MIN6 cells were seeded in the top well incubated with Cy3 and iPSCs in the bottom well. Fluorescence imaging in the top well demonstrated that the Cy3 was transfected successful into MIN6 cells. As MIN6 cells were not able to migrate through the 0.4 μ m porous membrane filter, the Cy3-labeled components the must have been transported and taken up into iPSCs as

red fluorescence was observed 48h later (Fig 2B, C). The robust consistency of the two experiments confirmed that MIN6 cell-derived exosomes successfully integrated and delivered their cargo into iPSCs.

Pancreatic marker genes expression in iPSCs with the induction of exosomes in the early stage

Exosomes were added to the medium to prepare the conditioned medium for iPSCs culture, without any other supplementation of known differentiation inducing factors. Exosomes induced the formation a cluster-like morphology of iPSCs and cell aggregates were observed at day 7 (Fig 3B).

We analyzed the expression of endocrine and β -cell specific genes as well as genes previously reported enriched during specific stages of pancreas development. Our results confirmed that insulin gene transcriptional activators, such as Mafa A and Ngn3 were significantly higher in exosome-induced iPSCs as compared to control cells. The expression of two transcription factors Foxa2 and Pdx1 critically involved in early pancreas development were also been analyzed. Indeed, we observed an increased expression of Foxa2 and a Pdx1 expression on day 5, while the expression levels of both transcription factors show a decreased trend on day 7. The mRNA for the hormone markers, Ins1, Ins2 and Gcg was found significantly higher in exosome-induced iPSCs than in control cells. In addition, Nkx6.1, Neurod1, SST, GCK and Isl1 showed a significant upregulation in the early stage of induction versus iPSCs without exosomal induction, demonstrating the endocrine pancreatic lineage commitment of these cells during the differentiation process. Unexpectedly, the expression of Glut2 were inconsistently with studies reported, demonstrating very low expression in the induced cells (data not shown). Totally, the genetic changes demonstrated that exosome induced iPSCs differentiation into insulin-producing cells specifically follows the steps of endocrine pancreas organogenesis. The typical embryonic/iPS stem cell marker Oct4 and endoderm marker Sox17 could be detected in iPSC clusters. However, there was no significant change in the expression of the two gene expression from day 3 to day 7 (Fig 3C). Primers were shown in Table 1.

FCM was performed to identify differentiation efficiency of insulin positive (insulin⁺) cells on day 7. The results showed that insulin⁺ cells were accounted for 22.3% compared to 11.9% in control cells without exosomes, nearly 2 fold as much (Fig 3D).

Table 1. Polymerase chain reaction primers sequences.

Gene	Sequence(5'-3')	
NGN3	F: CCTCTTCTGGCTTTCACTACTTG	R: GCGAGAGTTTGATGTGGCTG
Foxa2	F: GCATGGGACCTCACCTGAGT	R: CGAGTTCATGTTGGCGTAGG
MafaA	F: GGGAACGGTGATTGCTTAGG	R: ACTGCGCTCCACGTCTGTAC
Neurod1	F: CCAGGGTTATGAGATCGTC	R: GGTTCATGTTTCCACTTCCTG
GCG	F: TTTACTTTGTGGCTGGATTGCT	R: CTCTGTGTCTTGAAGGGCGT
SST	F: GAGAATGATGCCCTGGAGCC	R: TGTCTTCCAGAAGAAGTTCTTGC
GCK	F: TAAGGCACGAAGACATAGACAAGG	R: GCCACCACATCCATCTCAAAG
Ins1	F: ACTTCCTACCCCTGCTGG	R: ACCACAAAGATGCTGTTTGACA
Ins2	F: GCTTCTTCTACACCCCATGTC	R: AGCACTGATCTACAATGCCAC
Isl1	F: ATGATGGTGGTTTACAGGCTAAC	R: TCGATGCTACTTCACTGCCAG
Nkx6.1	F: CTGCACAGTATGGCCGAGATG	R: CCGGGTTATGTGAGCCCAA
Pdx1	F: CCTTCCCATGGATGAAGTC	R: CGTCCGCTTGTCTCCTC
OCT4	F: CAGTGCCCGAAACCCACAC	R: GGAGACCCAGCAGCCTCAAA
Sox17	F: GATGCGGGATACGCCAGTG	R: CCACCACCTCGCCTTTCAC
GAPDH	F: AGGTCGGTGTGAACGGATTTG	R: GGGGTCGTTGATGGCAACA

Immunofluorescence assays for Nkx6.1 and insulin in exosome induced iPSCs in the early stage

To further verify whether exosomes promoted specific protein expression in iPSCs, immunofluorescence for Nkx6.1 and insulin were performed. On day 3, almost no fluorescence were detected neither in exosome-induced cells nor in control cells. On day 5, both Nkx6.1 and insulin positively expressed in exosomes-induced iPSCs. On day 7, expression of insulin increased significantly compared to day 5 in exosomes-induced iPSCs (Fig 4).

Argonaut-2 (Ago2) inactivation in MIN6 cells weakens gene expression associated with differentiation

On day14, insulin positive cells were accounted using FCM. The results confirmed that insulin⁺ cells increased to 52.7% in the presence of exosomes compared to 22.4% of control group. Paralled with day 7, the insulin⁺ cells was about 2 fold higher as well (Fig 5A), which suggested that exosomes-derived molecules could induce insulin expression of iPSCs stably.

To test whether the increased gene expression was due to transfer of exosomal miRNAs, MIN6 cells were transfected with siRNA directed against Ago2. Ago2 knockdown efficiency was confirmed by qRT-PCR and Western blotting. The result revealed a 70% decrease in Ago2 mRNA and an approximately 50% decrease in Ago2 protein levels in MIN6 cells (Fig 5B&5C).

Most endocrine and β -cell specific genes expression as well as genes enriched during early stages were weakened since siAgo2 transfection (Fig 5D). Isl1, Ins2, Isl1, MafaA, GCG, GCK, Ngn3, SST were upregulated on day 14 and day 21 (except GCG) compared with control group. Nkx6.1 and Neurod1 expression were synchronous with MafaA in exosome-induced iPSCs. Significantly, we found that the expression of two transcription factors Foxa2 and Pdx1 critically involved in early pancreas development were downregulated in the late stages, while the expression of both genes show an increased expression in siAgo2-exosome-induced iPSCs on day14 and day21. In addition, the typical embryonic stem cell

marker Oct4 and endoderm marker Sox17 show a significant downregulation in iPSC clusters both on day14 and day21. Taken together, the results suggested that exosomes delivery stably induce iPSCs differentiation in vitro and mainly associated with miRNAs. Exosomal miRNAs form a novel class of signal molecules that mediate intercellular communication.

Immunofluorescence assays for glucagon and insulin expression in the late stage

Immunofluorescence for insulin and glucagon (a marker for α -cells) which is another islet cell type, were performed to verify the induction efficiency in vitro. We found that both insulin and glucagon were with weak positive signal in control cells. Additionally, there was no obvious cell morphological change, basically maintaining the original pleomorphic state of iPSCs cells. Surprisingly, both insulin and glucagon demonstrated a strong positive signal in exosome-induced iPSCs. Cells tended to gather and grow in clusters and became larger and rounder. While the two hormone marker were weakened in siAgo2-exosome-induced iPSCs, the morphology failed to be round. The results indicated that knockdown of Ago2 inhibited induction effect of exosomes in iPSCs, mainly through miRNA-dependent mechanisms (Fig 6A).

Differentially expressed microRNAs of MIN6 cell-derived exosomes and single-assay validation

Published work identified 24 miRNAs overlapping in two different miRNA sequencing datasets, among which 6 microRNAs were identified with high fold changes (MIN6 derived exosome versus MIN6 cells) (Fig 7A). The other 17 microRNAs were with lower expression in exosomes or almost equal representation in MIN6 parental cells. In order to confirm and validate the differential expression of those microRNAs identified, we analyzed the expression through qRT-PCR, miRNA information are listed in Table 2. The results demonstrated that miR-706 expressed gradually higher from day7 to day21, while in siAgo2-exosome induced iPSCs, the expression increased only on day7 and then decreased on the late stage. MiR-709 was upregulated significantly on day 14 and day21 compared to control group. The results showed an expression peak on day21. MiR-466c-5p demonstrated a similar expression pattern with miR-709. However, miR-423-5p showed its maximum upregulation in the early stage, and gradually decreased on the late stage. miR-1187 in siAgo2-exosome induced iPSCs was significantly reduced on day14 and day21. However, miR-1895 and miR-671-5p had no obvious change during differentiation (Fig 7B).

Table 2. List of miRNAs detected during differentiation stages in the experiment.

Gene name	Accession No.	Sequence(5'-3')
mmu-miR-466c-5p	MIMAT0004877	UGAUGUGUGUGUGCAUGUACAUAU
mmu-miR-1895	MIMAT0007867	CCCCCGAGGAGGACGAGGAGGA
mmu-miR-671-5p	MIMAT0003731	AGGAAGCCUGGAGGGGCUGGAG
mmu-miR-709	MIMAT0003499	GGAGGCAGAGGCAGGAGGA
mmu-miR-1187	MIMAT0005837	UAUGUGUGUGUGUAUGUGUGUAA
mmu-miR-706	MIMAT0003496	AGAGAAACCCUGUCUCAAAAAA
mmu-miR-423-5p	MIMAT0004825	UGAGGGGCAGAGAGCGAGACUUU

Differentiated insulin-producing cells improve glucose control capacity of experimental diabetic hyperglycemia in vivo

Non-fasting blood glucose was monitored to explore the functionality of differentiated insulin-producing cells. The results showed that the non-fasting blood glucose concentrations of control mice remained stable and normal, while blood glucose concentrations of the STZ +iPSCs group, STZ+exosome-induced iPSCs group and STZ+siAgo2-exosome-induced iPSCs showed much higher glucose levels (Fig 8A). Until iPSCs transplantation at day7, blood glucose concentration in both STZ+exosome-induced iPSCs group and STZ+siAgo2-exosome-induced iPSCs group showed a downward trend. It could be maintained stable for 14 days after transplantation in STZ+exosome-induced iPSCs animals, implying that the transplanted cells effectively controlled blood glucose levels. Although the concentration did not decrease to a normal level as reported, our results demonstrated a drop to half of the concentration (10mmol/L) compared to NC group. Meanwhile, STZ-treated mice exhibited progressively impaired glucose tolerance at day 7, 14 and 21, respectively. STZ+exosome-induced iPSCs group show a much better blood glucose control capacity compared to the other two groups at day14 and 21(Fig 8B).

Immunofluorescence for frozen kidney slices demonstrated that insulin expression in STZ+exosome-induced iPSCs group was significantly increased compared to the siAgo2-exosome group (Figure 8C), implying that the graft was functionally deficient, which further supported that knockdown of Ago2 significantly weakened exosomal miRNA function and affect differentiation.

Discussion

Common forms of diabetes (Type 1 and 2) are characterized by decreased β -cells and insulin deficiency^[25]. Current clinical treatments almost rely on daily insulin injections or the transplantation of cadaveric islets. However, the strategies are limited by drug tolerance, lack of donor sources, functionality of isolated islets or immune rejection. Therefore, to generate functional islet-like cells and restore insulin secretion is considered to be an effective approach for clinical treatments.

Published literatures have reported the application of iPSCs-based differentiation protocols for β -like cell regeneration^[26-31]. However, the differentiation efficiency of iPSCs are impaired by several technical or biological limitations, which may result in imperfect differentiation and immature insulin producing cells. As important epigenetic regulators, miRNAs have been reported to affect stem cell differentiation. Although microRNAs secreted by MIN6 cells into exosomes have been profiled in recent years^[32, 33], few work has specifically elucidated the distinct roles of exosomal miRNAs in iPSCs differentiation. Here, we established a novel and simplified protocol using MIN6 derived exosomes for iPSCs differentiation in vitro and explored the mechanisms.

Our initial data revealed the expression of genes related to endocrine pancreas development, such as mature endocrine cell specific genes *Ins1* (Insulin1), *Ins2* (Insulin2), *GCG* and *SST*, insulin gene transcriptional activators *Mafa A*, *NEUROD1* and *NGN3*, the transcription factors *Nkx6.1*, *Foxa2* and *Pdx1*.

Additionally, we analyzed the expression of GCK and Glut2 as part of glucose responsive machinery genes and stem cell specific gene Oct4 and Sox17. Among these genes, we found that expression of Nkx6.1 and Mafa A show a obvious upregulation on day3 compared to cells cultured in medium without exosomes. The other genes expression show significant differences at least on day5. Meanwhile, FCM detection further demonstrated that insulin⁺ cells were accounted for 22.3% on day7 and increased to 52.7% on day14. Based on these data, upregulation of the β -cell marker genes confirm the feasibility of exosome induction for iPSCs reprogramming. In addition, as previous study reported that insulin⁺ cells co-expressing Nkx6.1 can differentiate into functional β -cells following transplantation in vivo^[34, 35], we analyzed immunofluorescence staining for insulin and Nkx6.1 in iPSCs at different stages. Our results demonstrated that both insulin and Nkx6.1 feebly expressed on day3, but remarkably upregulated on day5 to day7. Instead, there was almost no immunofluorescence enhancement in iPSCs cultured without exosome. In this regard, we can speculate that exosomes indeed promote iPSCs differentiation into islet-like cells and promote insulin secretion, which indicates that MIN6 cell-derived exosomes have sufficiently high reprogramming efficiency for iPSCs.

In our studies reported here, siAgo2-exosomes from MIN6 cells poorly induced pancreatic related gene expression. Further support came from our studies in immunofluorescence assay for glucagon and insulin expression on day21 in vitro. Following differentiated β -like cells transplantation, we found the graft contributed to blood glucose control in the diabetic mice and improved the fasting blood glucose levels and glucose tolerance. The hyperglycemia in mice was attenuated, implying the functionality of transplanted cells in mice, although it was not downregulated to the normal level. Immunofluorescence for insulin in transplanted graft revealed that knockdown of Ago2 impaired insulin expression, indicating that the essential driving force for differentiation was dependent mostly on exosomal miRNAs from donor cells.

Two literatures performed MIN6 exosomal miRNA-seq were analyzed and 24 miRNAs were overlapped^[33, 36]. Among them, 6 microRNAs were with high fold changes, indicating that particular miRNAs were preferentially packaging into exosomes while others may selectively retain in parent MIN6 cells. Selective accumulation of specific miRNAs in exosomes released by other cell types was reported before^[37, 38]. MiR-709, miR-706 and miR-466c-5p were upregulated gradually from day7 to day21. The expression pattern of miR709 was in line with studies reported^[39], which was also been reported to inhibit adipocyte differentiation through targeting GSK3 β and subsequently activating Wnt/ β -catenin signaling pathway^[40]. On the contrary, miR-423-5p, reported associated with diabetes^[41-43], was downregulated gradually with the passage of induction time, which further underlined the exosomal-miRNA activity may need to be within a narrow range in regulating iPSCs differentiation. However, miR-671-5p and miR-1187 did not show significantly change. Based on our data, 4 exosomal microRNAs (miR-706, miR-709, miR-466c-5p and miR-423-5p) actively modulating iPSCs differentiation. Therefore, it is worthy of our focus on these microRNAs in the future research.

Undeniably, our findings confirmed that iPSCs differentiation into functional pancreatic β -like cells through delivery of exosomes was effective and feasible, although the present study was unable to delineate the exact mechanisms of miRNA interaction network or identify dominant miRNAs involved in the mechanism. On the other hand, the population of insulin⁺ cells induced with exosomes in vitro achieved 52.7% on the middle differentiation stage, which was higher than our previous methods^[24]. However, hyperglycemia in mice was downregulated only partially. The decreased endocrine function after cell transplantation may due to the lack of optimized differentiation microenvironment in vivo. Although β -cell differentiation is a complex and highly regulated process, our findings provide greater insights into the roles of exosomal miRNAs. Our findings encourage us to concentrate on refinement of exosome induction scheme, such as pancreatic acellular scaffold apply, to further improve differentiation efficiency, as well as reveal the function and mechanism of exosomal miRNAs in a more detailed and systematic way.

Declarations

Funding This work was supported by Project funded by China Postdoctoral Science Foundation (2019M661904), Postdoctoral program funded by Jiangsu province (2019Z154).

Author contributions Qingsong Guo, Yan Huang, Jia Luo conceived and designed the research. Qingsong Guo, Yuhua Lu, Yibing Guo, Shajun Zhu, Qiuqiang Zhang and Donghui Zhu performed the experiments. All authors analysed the data and edited and revised the manuscript. Jia Luo and Zhiwei Wang are the guarantors of this work.

Conflict

The authors indicate no potential conflicts of interest.

References

1. A. Rezaia, J. Bruin, P. Arora, A. Rubin, I. Batushansky, A. Asadi, S. O'Dwyer, N. Quiskamp, M. Mojibian, T. Albrecht, Y. Yang, J. Johnson, T. Kieffer, Reversal of diabetes with insulin-producing cells derived in vitro from human pluripotent stem cells. *Nature biotechnology*. **32**(11), 1121–1133 (2014)
2. A. Sinclair, P. Saeedi, A. Kaundal, S. Karuranga, B. Malanda, R. Williams, Diabetes and global ageing among 65-99-year-old adults: Findings from the International Diabetes Federation Diabetes Atlas, 9 edition. *Diabetes research and clinical practice*. **162**, 108078 (2020)
3. X. He, Y. Zhang, Y. Zhou, C. Dong, J. Wu, Direct Medical Costs of Incident Complications in Patients Newly Diagnosed With Type 2 Diabetes in China. *Diabetes therapy: research, treatment and education of diabetes and related disorders*. **12**(1), 275–288 (2021)
4. M. Bellin, F. Barton, A. Heitman, J. Harmon, R. Kandaswamy, A. Balamurugan, D. Sutherland, R. Alejandro, B. Hering, Potent induction immunotherapy promotes long-term insulin independence after islet transplantation in type 1 diabetes. *American journal of transplantation: official journal of the*

- American Society of Transplantation and the American Society of Transplant Surgeons. **12**(6), 1576–1583 (2012)
5. A. Shapiro, J. Lakey, E. Ryan, G. Korbitt, E. Toth, G. Warnock, N. Kneteman, R. Rajotte, Islet transplantation in seven patients with type 1 diabetes mellitus using a glucocorticoid-free immunosuppressive regimen. *The New England journal of medicine*. **343**(4), 230–238 (2000)
 6. A. Croon, R. Karlsson, C. Bergström, E. Björklund, C. Möller, L. Tydén, A. Tibell. Lack of donors limits the use of islet transplantation as treatment for diabetes. *Transplantation proceedings*. **35**(2):764 (2003)
 7. M. Williams, M. Joglekar, S. Satoor, W. Wong, E. Keramidaris, A. Rixon, P. O'Connell, W. Hawthorne, G. Mitchell, A. Hardikar, Epigenetic and Transcriptome Profiling Identifies a Population of Visceral Adipose-Derived Progenitor Cells with the Potential to Differentiate into an Endocrine Pancreatic Lineage. *Cell transplantation*. **28**(1), 89–104 (2019)
 8. Q. Zhou, D. Melton, Pancreas regeneration. *Nature*. **557**(7705), 351–358 (2018)
 9. T. Katsuda, T. Ochiya, Molecular signatures of mesenchymal stem cell-derived extracellular vesicle-mediated tissue repair. *Stem cell research & therapy*. **6**, 212 (2015)
 10. S. Moradi, S. Asgari, H. Baharvand, Concise review: harmonies played by microRNAs in cell fate reprogramming. *Stem cells (Dayton, Ohio)*. **32**(1), 3–15 (2014)
 11. R. Bashratyan, H. Sheng, D. Regn, M. Rahman, Y. Dai, Insulinoma-released exosomes activate autoreactive marginal zone-like B cells that expand endogenously in prediabetic NOD mice. *European journal of immunology*. **43**(10), 2588–2597 (2013)
 12. C. Castaño, A. Novials, M. Párrizas, Exosomes and diabetes. *Diabetes/metabolism research and reviews*. **35**(3), e3107 (2019)
 13. F. Pardo, R. Villalobos-Labra, B. Sobrevia, F. Toledo, L. Sobrevia, Extracellular vesicles in obesity and diabetes mellitus. *Molecular aspects of medicine*. **60**, 81–91 (2018)
 14. J. Li, C. Tong, T. Sung, T. Kang, X. Zhou, C. Liu, CMEP: a database for circulating microRNA expression profiling. *Bioinformatics (Oxford, England)*. **35**(17), 3127–3132 (2019)
 15. M. LaPierre, M. Stoffel, MicroRNAs as stress regulators in pancreatic beta cells and diabetes. *Molecular metabolism*. **6**(9), 1010–1023 (2017)
 16. A. Zhang, D. Li, Y. Liu, J. Li, Y. Zhang, C. Zhang, Islet β cell: An endocrine cell secreting miRNAs. *Biochemical and biophysical research communications*. **495**(2), 1648–1654 (2018)
 17. L. Eliasson, The small RNA miR-375 - a pancreatic islet abundant miRNA with multiple roles in endocrine beta cell function. *Molecular and cellular endocrinology*. **456**, 95–101 (2017)
 18. M. Kaviani, N. Azarpira, M. Karimi, I. Al-Abdullah, The role of microRNAs in islet β -cell development. *Cell biology international*. **40**(12), 1248–1255 (2016)
 19. M. Ha, V. Kim, Regulation of microRNA biogenesis. *Nature reviews. Molecular cell biology*. **15**(8), 509–524 (2014)

20. S. Tattikota, T. Rathjen, S. McAnulty, H. Wessels, I. Akerman, M. van de Bunt, J. Hausser, J. Esguerra, A. Musahl, A. Pandey, X. You, W. Chen, P. Herrera, P. Johnson, D. O'Carroll, L. Eliasson, M. Zavolan, A. Gloyn, J. Ferrer, R. Shalom-Feuerstein, D. Aberdam, M. Poy, Argonaute2 mediates compensatory expansion of the pancreatic β cell. *Cell metabolism*. **19**(1), 122–134 (2014)
21. J. Guduric-Fuchs, A. O'Connor, B. Camp, C. O'Neill, R. Medina, D. Simpson, Selective extracellular vesicle-mediated export of an overlapping set of microRNAs from multiple cell types. *BMC genomics*. **13**, 357 (2012)
22. Y. Zhang, M. Chopp, X. Liu, M. Katakowski, X. Wang, X. Tian, D. Wu, Z. Zhang, Exosomes Derived from Mesenchymal Stromal Cells Promote Axonal Growth of Cortical Neurons. *Molecular neurobiology*. **54**(4), 2659–2673 (2017)
23. B. Mead, S. Tomarev, Bone Marrow-Derived Mesenchymal Stem Cells-Derived Exosomes Promote Survival of Retinal Ganglion Cells Through miRNA-Dependent Mechanisms. *Stem cells translational medicine*. **6**(4), 1273–1285 (2017)
24. Y. Xu, Y. Huang, Y. Guo, Y. Xiong, S. Zhu, L. Xu, J. Lu, X. Li, J. Wan, Y. Lu, Z. Wang, microRNA-690 regulates induced pluripotent stem cells (iPSCs) differentiation into insulin-producing cells by targeting Sox9. *Stem cell research & therapy*. **10**(1), 59 (2019)
25. J. Flannick, J. Florez, Type 2 diabetes: genetic data sharing to advance complex disease research. *Nature reviews. Genetics*. **17**(9), 535–549 (2016)
26. K. Jeon, H. Lim, J. Kim, N. Thuan, S. Park, Y. Lim, H. Choi, E. Lee, J. Kim, M. Lee, S. Cho, Differentiation and transplantation of functional pancreatic beta cells generated from induced pluripotent stem cells derived from a type 1 diabetes mouse model. *Stem cells and development*. **21**(14), 2642–2655 (2012)
27. Y. Kondo, T. Toyoda, R. Ito, M. Funato, Y. Hosokawa, S. Matsui, T. Sudo, M. Nakamura, C. Okada, X. Zhuang, A. Watanabe, A. Ohta, N. Inagaki, K. Osafune, Identification of a small molecule that facilitates the differentiation of human iPSCs/ESCs and mouse embryonic pancreatic explants into pancreatic endocrine cells. *Diabetologia*. **60**(8), 1454–1466 (2017)
28. P. Mandal, D. De, K. Yun, K. Kim, Improved differentiation of human adipose stem cells to insulin-producing β -like cells using PDGFR kinase inhibitor Tyrphostin9. *Biochemical and biophysical research communications*. **533**(1), 132–138 (2020)
29. I. Schroeder, A. Rolletschek, P. Blyszczuk, G. Kania, A. Wobus, Differentiation of mouse embryonic stem cells to insulin-producing cells. *Nature protocols*. **1**(2), 495–507 (2006)
30. H. Xu, K. Tsang, J. Chan, P. Yuan, R. Fan, H. Kaneto, G. Xu, The combined expression of Pdx1 and MafA with either Ngn3 or NeuroD improves the differentiation efficiency of mouse embryonic stem cells into insulin-producing cells. *Cell transplantation*. **22**(1), 147–158 (2013)
31. K. Oh, S. Kim, D. Kim, M. Seo, C. Lee, H. Lee, J. Oh, E. Choi, D. Lee, Y. Gho, K. Park, In Vivo Differentiation of Therapeutic Insulin-Producing Cells from Bone Marrow Cells via Extracellular Vesicle-Mimetic Nanovesicles. *ACS nano*. **9**(12), 11718–11727 (2015)

32. D. Li, W. Zhang, X. Chen, H. Ling, P. Xie, Z. Chen, A. Adili, Z. Chen, F. Yang, C. Zhang, X. Jiang, J. Li, Y. Zhang, Proteomic profiling of MIN6 cell-derived exosomes. *Journal of proteomics*. **224**, 103841 (2020)
33. P. Mandal, D. De, D. Im, S. Um, K. Kim, Exosome-Mediated Differentiation of Mouse Embryonic Fibroblasts and Exocrine Cells into β -Like Cells and the Identification of Key miRNAs for Differentiation. *Biomedicines*. **8**(11) (2020)
34. F. Pan, M. Brissova, Pancreas development in humans. *Current opinion in endocrinology, diabetes, and obesity*. **21**(2):77–82 (2014)
35. J. Ray, K. Kener, B. Bitner, B. Wright, M. Ballard, E. Barrett, J. Hill, L. Moss, J. Tessem, Nkx6.1-mediated insulin secretion and β -cell proliferation is dependent on upregulation of c-Fos. *FEBS letters*. **590**(12), 1791–1803 (2016)
36. C. Guay, V. Menoud, S. Rome, R. Regazzi, Horizontal transfer of exosomal microRNAs transduce apoptotic signals between pancreatic beta-cells. *Cell communication and signaling: CCS*. **13**, 17 (2015)
37. H. Valadi, K. Ekström, A. Bossios, M. Sjöstrand, J. Lee, J. Lötvall, Exosome-mediated transfer of mRNAs and microRNAs is a novel mechanism of genetic exchange between cells. *Nature cell biology*. **9**(6), 654–659 (2007)
38. Y. Gon, S. Maruoka, T. Inoue, K. Kuroda, K. Yamagishi, Y. Kozu, S. Shikano, K. Soda, J. Lötvall, S. Hashimoto, Selective release of miRNAs via extracellular vesicles is associated with house-dust mite allergen-induced airway inflammation. *Clinical and experimental allergy: journal of the British Society for Allergy and Clinical Immunology*. **47**(12), 1586–1598 (2017)
39. S. Surendran, V. Jideonwo, C. Merchun, M. Ahn, J. Murray, J. Ryan, K. Dunn, J. Kota, N. Morral, Gene targets of mouse miR-709: regulation of distinct pools. *Scientific reports*. **6**, 18958 (2016)
40. J. Zhang, F. Zhang, X. Didelot, K. Bruce, F. Cagampang, M. Vatish, M. Hanson, H. Lehnert, A. Ceriello, C. Byrne, Maternal high fat diet during pregnancy and lactation alters hepatic expression of insulin like growth factor-2 and key microRNAs in the adult offspring. *BMC genomics*. **10**, 478 (2009)
41. S. Garavelli, S. Bruzzaniti, E. Tagliabue, F. Prattichizzo, D. Di Silvestre, F. Perna, L. La Sala, A. Ceriello, E. Mozzillo, V. Fattorusso, P. Mauri, A. Puca, A. Franzese, G. Matarese, M. Galgani, P. de Candia, Blood Co-Circulating Extracellular microRNAs and Immune Cell Subsets Associate with Type 1 Diabetes Severity. *International journal of molecular sciences*. **21**(2) (2020)
42. Y. Xu, J. Zhang, L. Fan, X. He, miR-423-5p suppresses high-glucose-induced podocyte injury by targeting Nox4. *Biochemical and biophysical research communications*. **505**(2), 339–345 (2018)
43. W. Yang, J. Wang, Z. Chen, J. Chen, Y. Meng, L. Chen, Y. Chang, B. Geng, L. Sun, L. Dou, J. Li, Y. Guan, Q. Cui, J. Yang, NFE2 Induces miR-423-5p to Promote Gluconeogenesis and Hyperglycemia by Repressing the Hepatic FAM3A-ATP-Akt Pathway. *Diabetes*. **66**(7), 1819–1832 (2017)

Figures

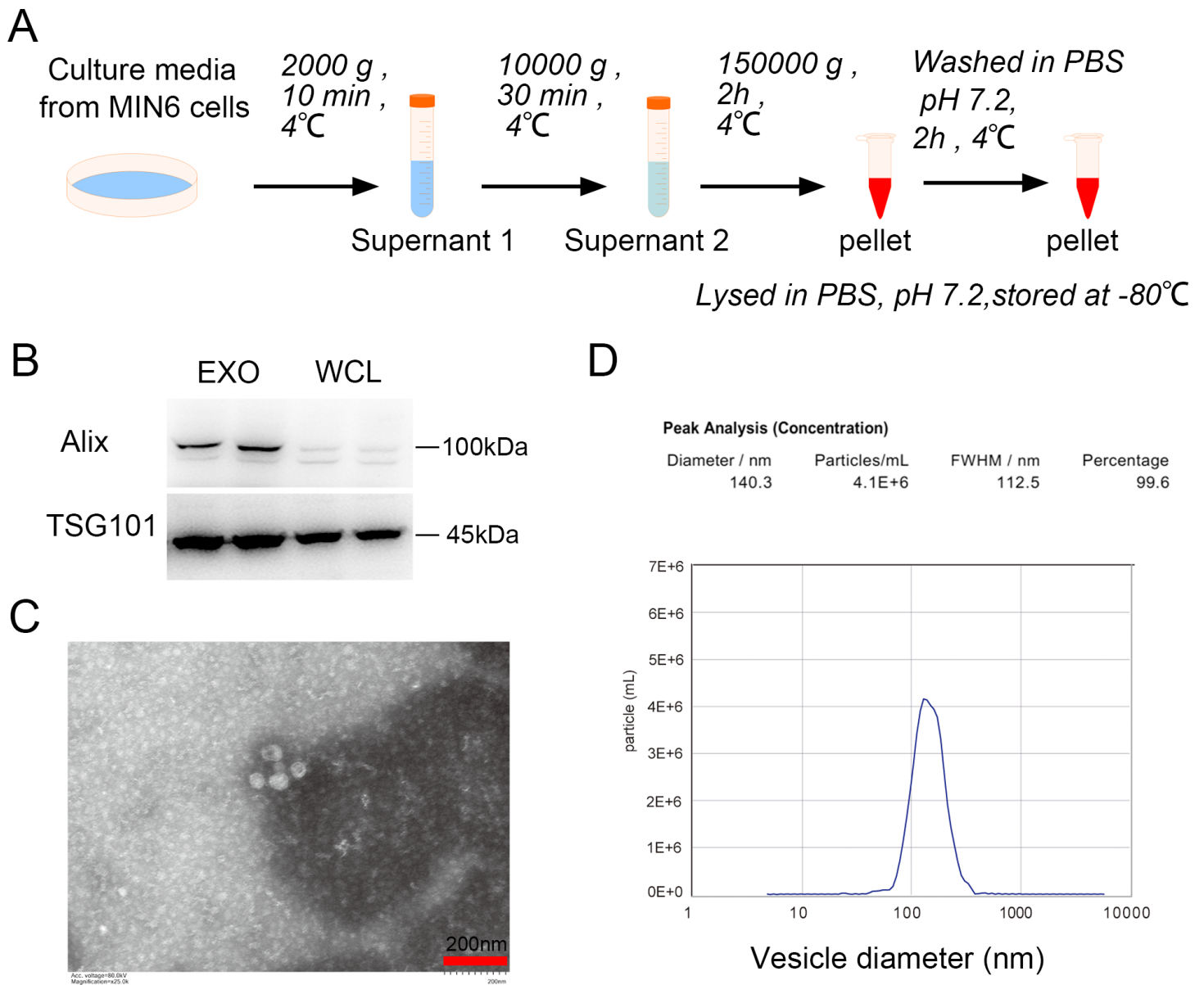


Figure 1

Exosomes isolation and characterization. A. Scheme of exosome ultra-centrifugation from MIN6 cells culture media. B. Western blot analysis of Alix and TSG101, Whole cell lysates (WCL) of MIN6 cells were loaded as controls. C. Representative TEM image. Scale bar =200 nm. D. Size distribution detection by NTA.

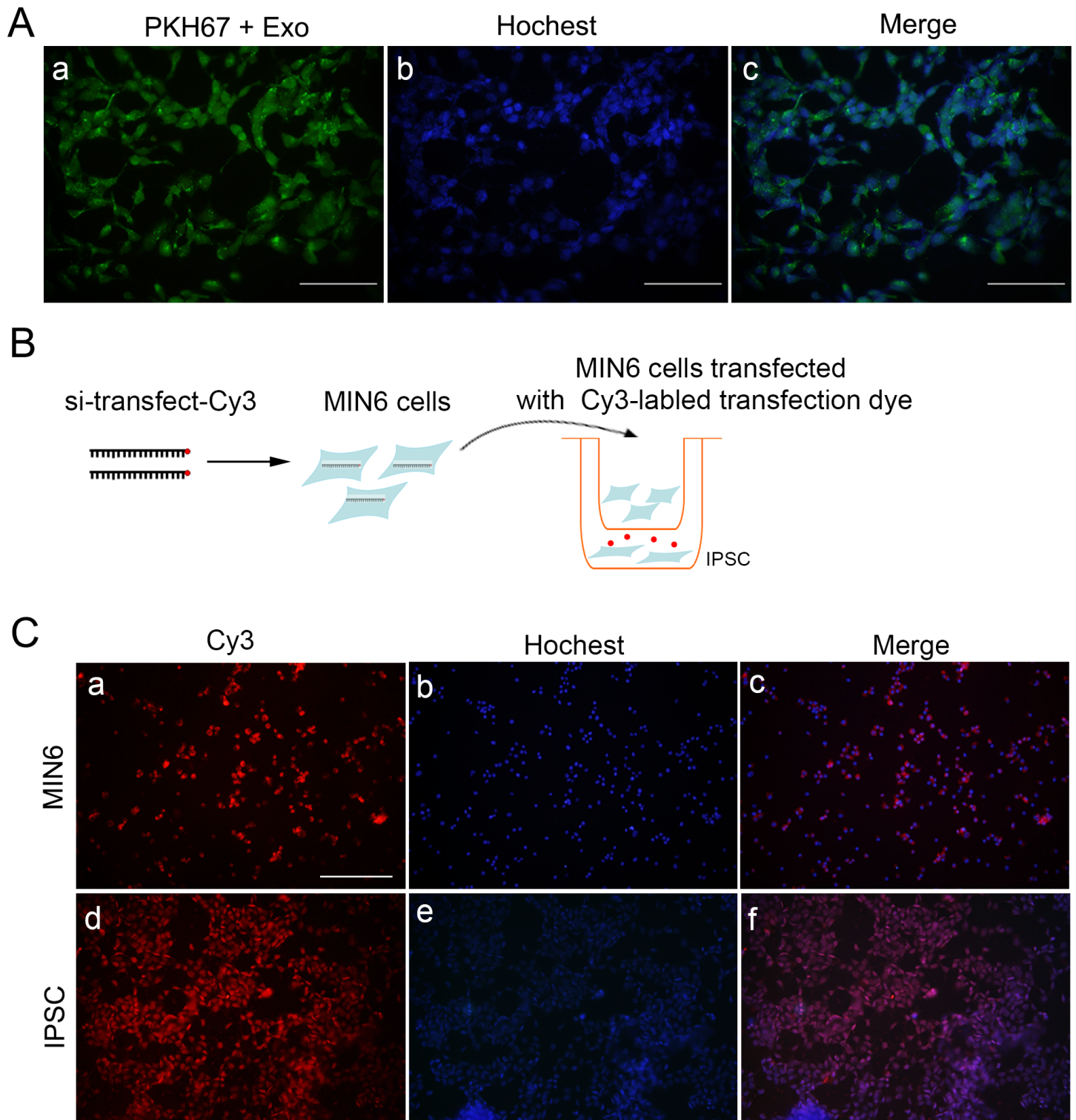


Figure 2

Exosomes purified from MIN6 cells were uptaken by iPSCs. A. Exosomes released by MIN6 cells were labeled with PKH67 and green fluorescence were observed in iPSCs 24h after incubation, scale bar = 50µm. B. Diagram for transwell experiment. C. Fluorescence were detected for MIN6 cells in the top well (a-c) and iPSCs in the bottom well (d-f), scale bar = 100µm. Hoechst was applied for nuclei staining.

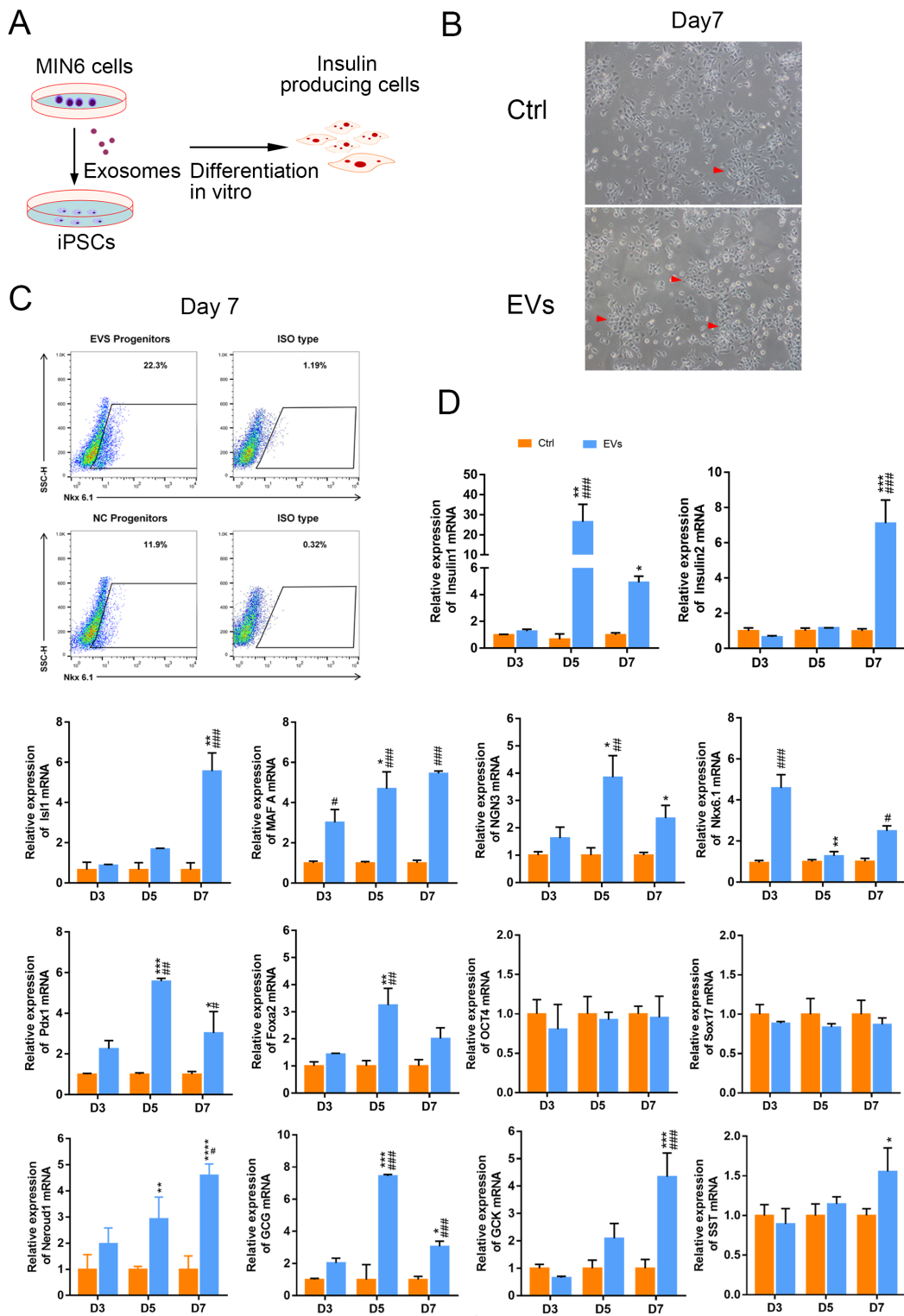


Figure 3

iPSCs morphologies, number of insulin+ cells and quantitative RT-PCR analysis of key genes in the early induction stage. A. Schematic diagram of the experiment. B. Bright-field images of iPSCs morphology induced with exosomes, red arrows indicate the cell clusters, scale bar = 100 μ m. C. Flow cytometry detection on day7. D. Expression of selected endocrine and beta cell specific genes, including insulin1, insulin2, Isl1, Mafa A, Ngn3, Nkx6.1, Neurod1, Pdx1, Foxa2, Gcg, Gck, Sst and stem cell marker Oct4 and

Sox17 in iPSCs. GAPDH was used as the internal control. Error bars show mean \pm SD (n=3). Compared with day3,*p<0.05, **p< 0.01, ***p< 0.001, ****p< 0.001; Compared with the control group on the same day , #p<0.05, ##p<0.01, ###p<0.001, ####p<0.0001.

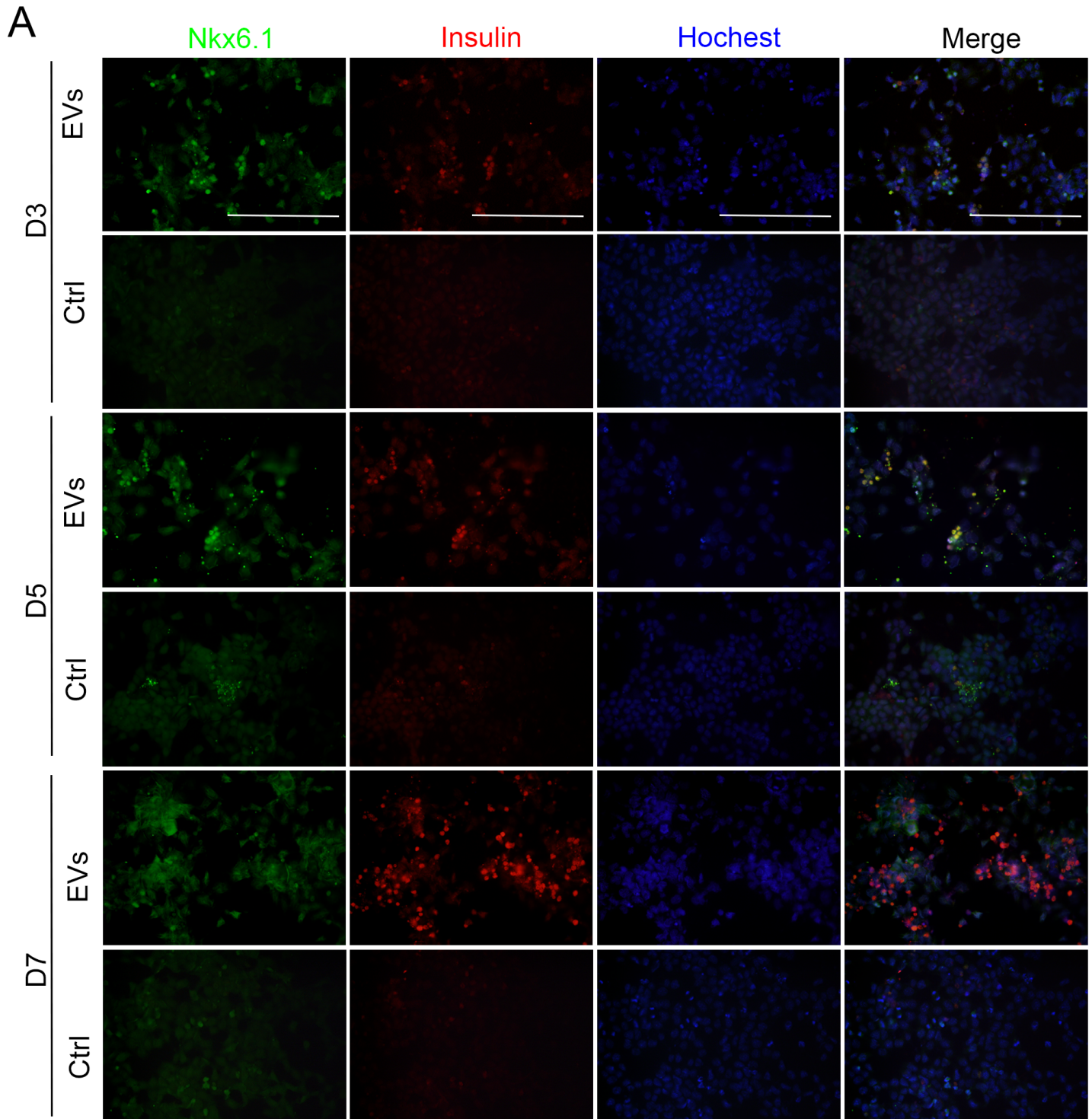


Figure 4

Immunofluorescence assays for Nkx6.1 and insulin expression. A. Representative images of co-immunostaining of Nkx6.1 (green) and insulin (red), nuclear hochest staining is shown in blue, scale bar = 50 μ m.

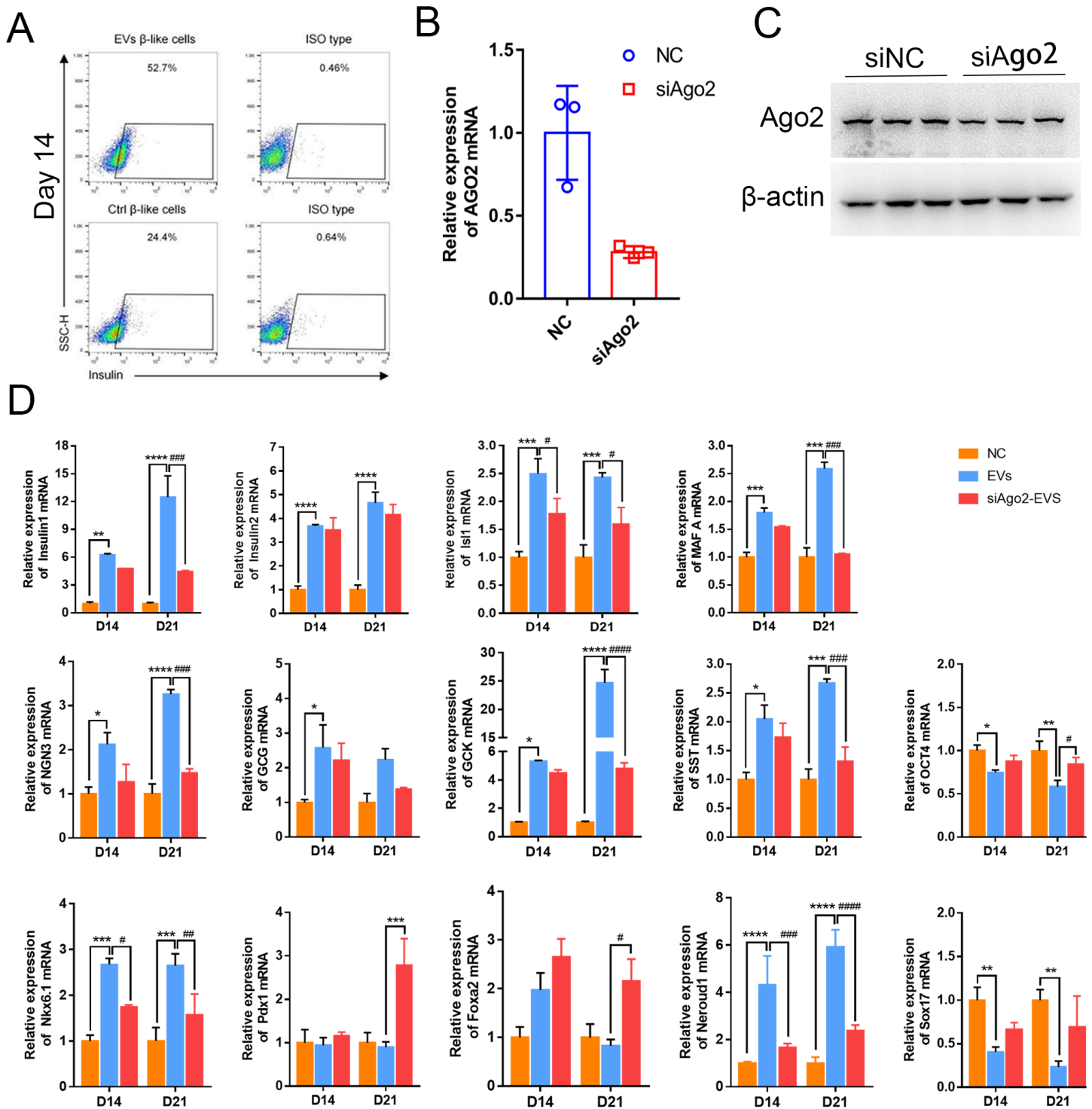


Figure 5

Quantitative RT-PCR analysis of the key genes and flow cytometry for insulin+ cells on the late induction stage. A. Flow cytometry detection on day14. B. Efficiency for Ago2 knockdown was confirmed by qRT-PCR. C. Efficiency for Ago2 knockdown was confirmed by Western blotting. D. Expression of selected endocrine and beta cell specific genes, including *Ins1*, *Ins2*, *Isl1*, *Mafa A*, *Ngn3*, *Nkx6.1*, *Neurod1*, *Pdx1*, *Foxa2*, *Gcg*, *Gck*, *Sst* and stem cell marker *Oct4* and *Sox17* during the exosome-induced late stage. GAPDH was used as the internal control. Error bars show mean \pm standard deviation (SD) (n=3).

Compared with day 14,*p<0.05, **p< 0.01, ***p< 0.001, ****p< 0.001; Compared with the control group on the same day , #p<0.05, ##p<0.01, ###p<0.001, ####p<0.0001.

A

*Claudiane Guay
et al, 2015*



*Paulami Mandal
et al, 2020*

mmu-miR-324-3p
mmu-miR-345-5p
mmu-miR-466c-5p
mmu-miR-532-3p
mmu-miR-342-3p
mmu-miR-465a-3p
mmu-miR-1895
mmu-miR-466f-3p

mmu-miR-129-2-3p
mmu-miR-125a-5p
mmu-miR-671-5p
mmu-miR-324-5p
mmu-miR-709
mmu-miR-532-5p
mmu-miR-574-5p
mmu-miR-1187

mmu-miR-384-5p
mmu-miR-340-5p
mmu-miR-129-5p
mmu-miR-706
mmu-miR-125b-5p
mmu-miR-384-3p
mmu-miR-467f
mmu-miR-423-5p

B

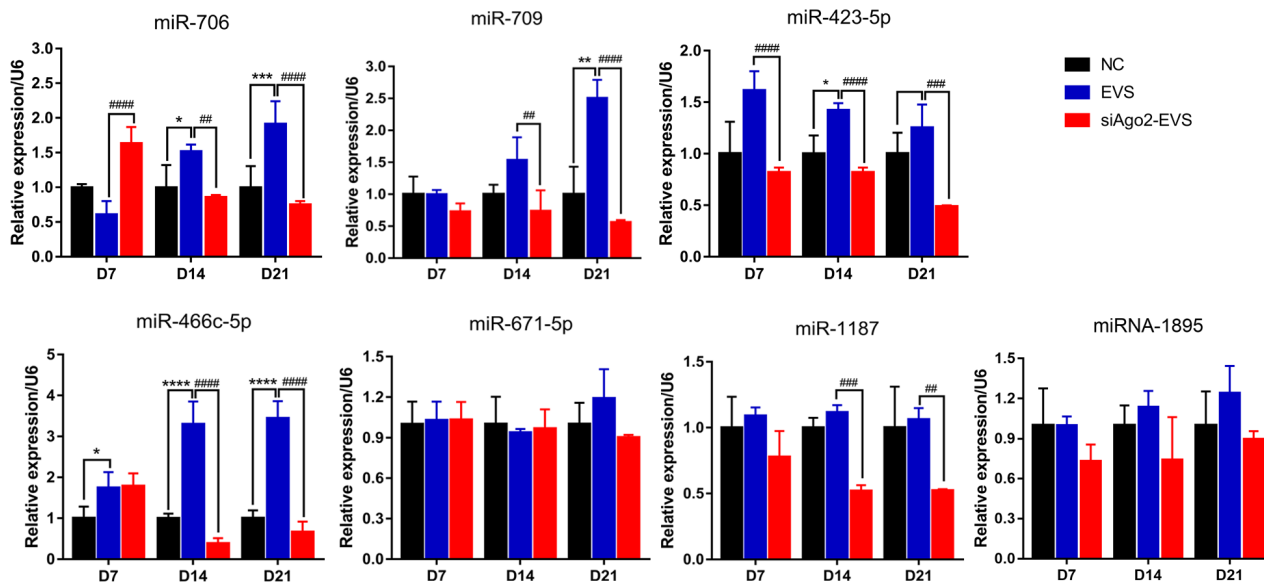


Figure 6

Immunofluorescence assays for glucagon and insulin expression of differentiated iPSCs at day21. A. Representative images of co-immunostaining of glucagon (green) and insulin (red), nuclear hochest staining is shown in blue, scale bar = 50µm.

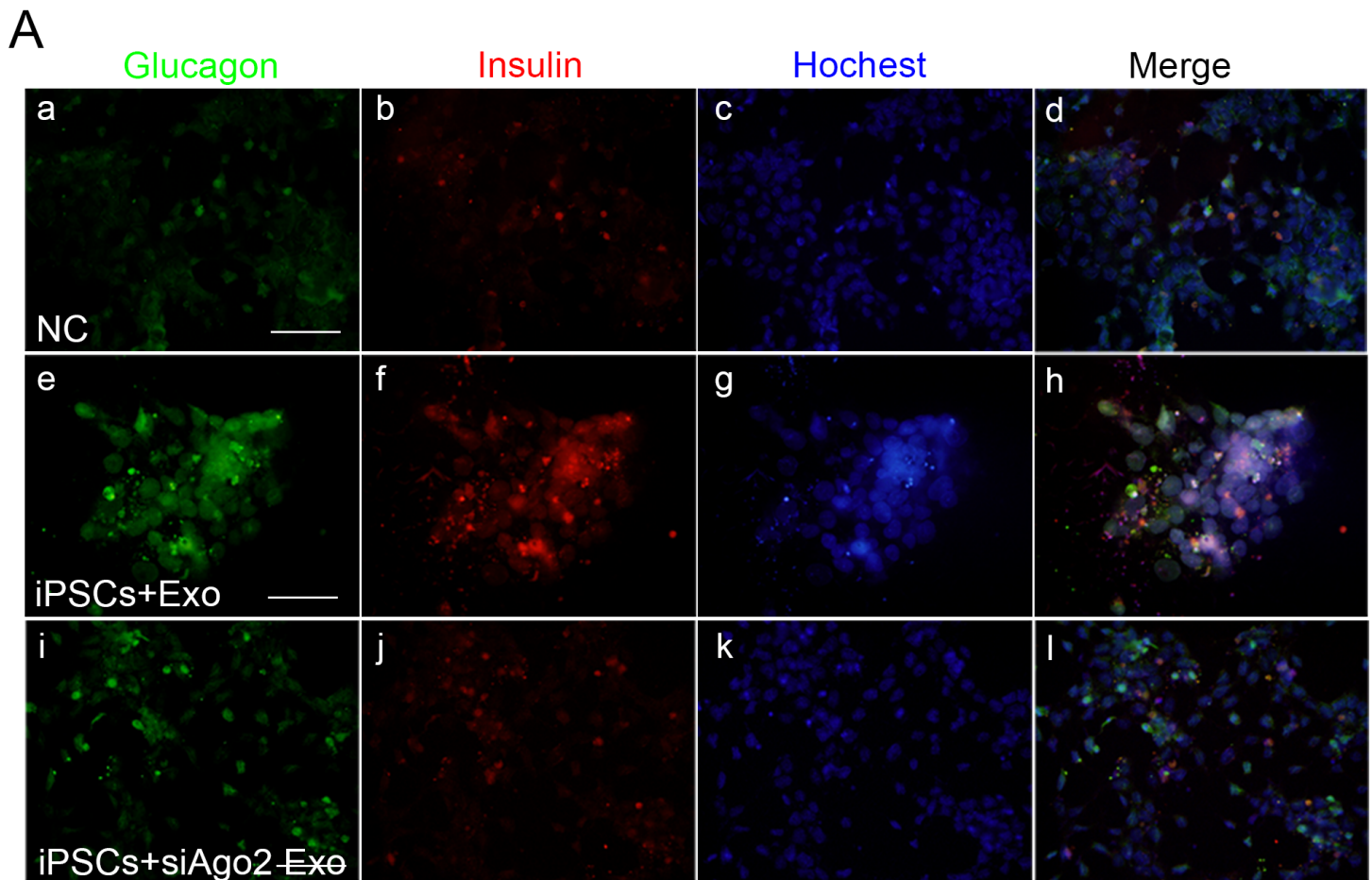


Figure 7

Common expressed miRNAs screening in exosomes and single-assay validation. A. Venn diagram presented exosomal miRNAs sequenced from two reported MIN6 exosomes. 7 highly expressed miRNAs in exosomes (fold change >10) among the 24 miRNAs were validated. Cells shaded in red or blue highlighted indicated the miRNAs reported associated with stem cell differentiation. B. Single-assay validation of miRNAs with quantitative RT-PCR. Error bars show mean \pm SD (n=3). Compared with day7, *p<0.05, **p< 0.01, ***p< 0.001, ****p< 0.0001; Compared with NC group on the same day , #p<0.05, ##p<0.01, ###p<0.001, ####p<0.0001.

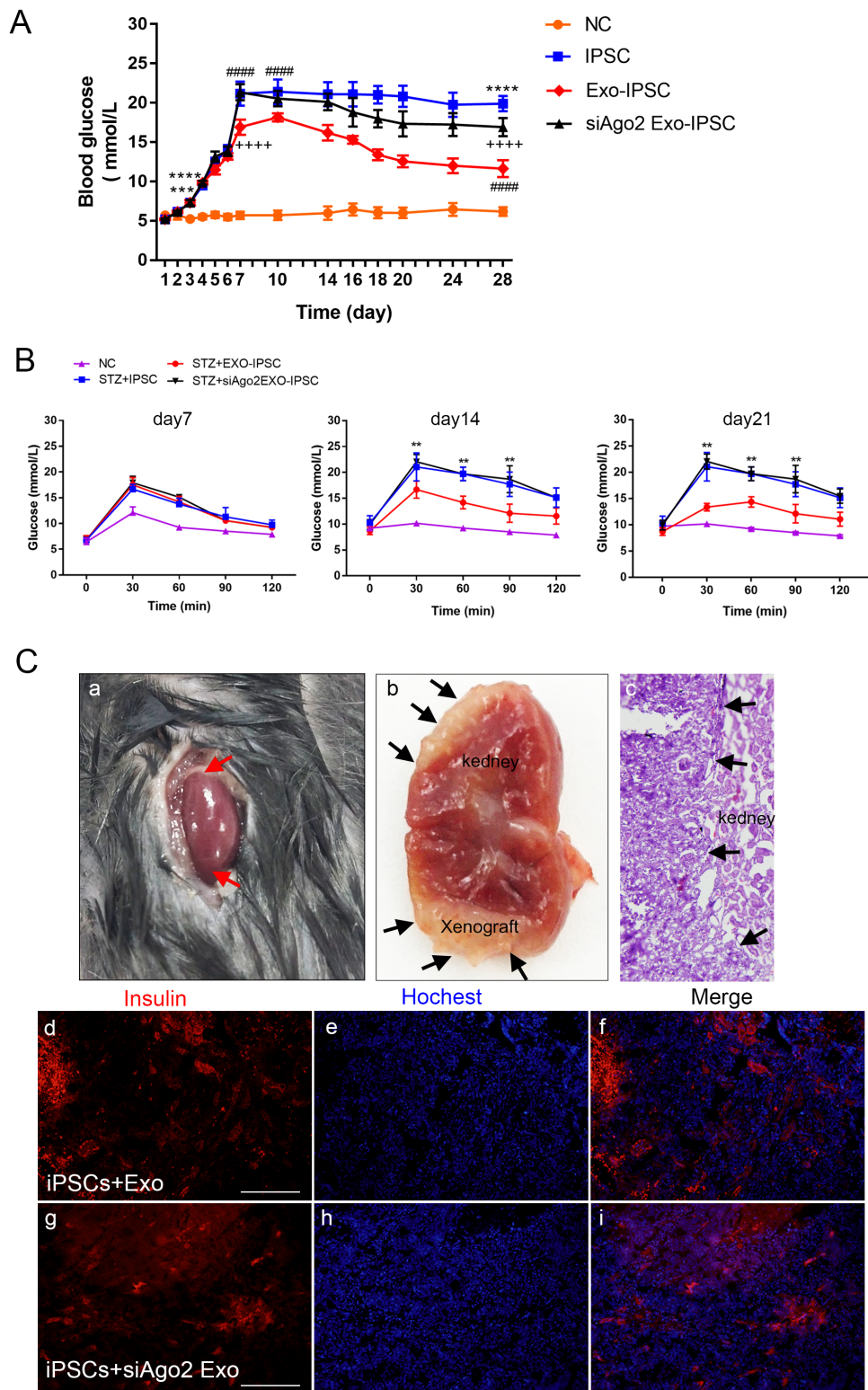


Figure 8

Transplantation of differentiated iPSCs into STZ pre-treated C57BL/6J mice. A. Non-fasting blood glucose concentrations of STZ +iPSCs group, STZ+exosome-induced iPSCs and STZ+siAgo2-exosome-induced iPSCs(n=8); NC group, n=5; B. Intraperitoneal glucose tolerance tests (IPGTT) were performed on day 7, day 14 and day 21. C. HE staining and immunofluorescence detection for insulin (red) at day28 after transplantation. Data were showed as mean \pm SD, compared with NC group, * $P < 0.05$, ** $P < 0.01$,

***P<0.001; compared with iPSCs group, #p<0.05, ##p<0.01, ###p<0.001, ####p<0.0001; compared with exosome group, +p<0.05, ++p<0.01, +++p<0.001, ++++p<0.0001. Scale bar =50µm. Abbreviations: IPGTT, intraperitoneal glucose tolerance test; STZ, streptozotocin.